ISSN (Print) 1226-1750
ISSN (Online) 2233-6656
**Journal of Magnetics** 24(3), 379-391 (2019) https://doi.org/10.4283/JMAG.2019.24.3.379

# Magnetic Effects on Second Grade Fluid Flow due to Non Coaxial Rotation of a Disk Through a Porous Medium with Double Diffusion

**Ahmad Qushairi Mohamad[1], Ilyas Khan[2]*, and Sharidan Shafie[1]**

[1]*Department of Mathematical Sciences, Faculty of Science, Universiti Teknologi Malaysia, 81310 Johor Bahru, Malaysia*
[2]*Faculty of Mathematics and Statistics, Ton Duc Thang University, Ho Chi Minh City, Vietnam*

(Received 16 September 2018, Received in final form 25 June 2019, Accepted 25 June 2019)

**In this paper, the unsteady of magnetohydrodynamics (MHD) second grade fluid in a porous medium due to non–coaxial rotation is investigated. The effects of heat and mass transfers (double diffusion) through an oscillating disk are considered. The non–dimensional governing momentum, energy and mass equations are obtained by using the suitable non–dimensional variables. The Laplace transform method is used to obtain the exact solutions of non–dimensional velocity, temperature and concentration profiles. The expressions of skin friction, Nusselt number and Sherwood number are also presented. The numerical result for all fluid flow profiles are plotted in graphs for the different parameters studied. The results also show that, velocity for present solution (with heat and mass transfers) has a significant impact on the velocity profiles in non-coaxial rotation due to exhibits high thermal diffusivity and thermal conductivity. The obtained exact solutions are found to be identical to the Guria [10]. It is worth mentioning that, the exact solutions are in excellent agreement with the numerical solutions of Inverse Laplace transform obtained by Gaver-Stehfest algorithm.**

**Keywords :** Non-coaxial rotation, heat and mass, second grade fluid, MHD, porous medium, Laplace transform

## 1. Introduction

Magnetohydrodynamic (MHD) is the study of the dynamic of a conducting fluid in the presence of magnetic field. MHD is of great important in many areas of geophysics, technology, astrophysics and fluid engineering. For example, MHD power generation, MHD pumps, aerodynamic heating, application in the flow of liquid metals and alloys, purification of crude oil and fluid droplets, petroleum industry, cardiology and also application in flow of mercury amalgams. The investigation of the MHD rotation flow has gained extensive attention of researches due to the wide range of application in fluid engineering and geophysics astrophysics. A force called Coriolis force is generated due to the rotation and it has a significant effect on the MHD flow. A number of researchers have considered the viscous incompressible flow due to non-coaxial rotations of a disk and a fluid at infinity. The possibility of an exact solution for the flow was implied by Berker [1]. Coirier [2] studied the flow by considering that the disk and the fluid at infinity rotate non-coaxially at a slightly different angular velocity. Erdogan [3] extended the work of Coirier [2] for the case of a porous disk. The investigation of the MHD flow due to eccentric rotations of a porous disk and a fluid at infinity has been done by Murthy and Ram [4]. A simple fluid flow in an orthogonal rheometer has been studied by Rajagopal [5]. Kasiviswanathan and Rao [6] presented an exact solution for the unsteady Newtonian fluid flow due to non-coaxial rotations of a porous disk oscillating in its own plane and the fluid at infinity. Recently, by mean of Laplace transform methods, an exact solution of the unsteady MHD flow due to non-coaxial rotations of a porous disk and a fluid at infinity on taking Hall currents into account has been obtained by Guria [7]. Asghar [8] studied the effect of slip condition on the flow due to eccentric rotations of fluid at infinity and a porous disk. Hayat [9] examined the effect of Hall current on the MHD flow due to non-coaxial rotations of an oscillating porous disk and a fluid at infinity. Guria [10] extended the work done by Guria [7] by considering the effect of slip condition on the porous disk. Due to the great important of flows through porous medium in petroleum engineering and chemical engineering, Maji [11] studied the unsteady MHD flow


*Corresponding author: Tel: +503346170
Fax: +009662601, e-mail: ilyaskhan@tdtu.edu.vn

due to non-coaxial rotations of a porous disk and a fluid at infinity through a porous medium. They found that the fluid flow takes more time to reach the steady state in case of porosity than the case of no porosity of the medium. Further, Mohamad [12] investigated the unsteady free convection flow of Newtonian fluid due to non-coaxial rotation of an oscillating vertical plate with constant wall temperature and a fluid at infinity. They have considered the heat transfer in the Newtonian fluid and the study is important in many areas, such as automatic control systems, cooling turbine blade and in designing thermal syphon tubes. Recently, the combined effects of heat and mass transfer on mixed convection flow of an incompressible viscous fluid through an oscillating infinite vertical disk with eccentric rotation and a fluid at infinity has been studied by Mohamad [13].

In all the above studies, there is a lacuna that non-Newtonian fluid was not considered by the authors. Non-Newtonian fluid is a type of fluid that does not obey Newton's law of viscosity. The fluid may have variable viscosity at a constant temperature and also the viscosity is dependent on the applied force. Syrupy mixture of corn-starch and water, quicksand, slurries, pastes, gels and polymer are same examples of the non-Newtonian fluid. Coleman and Noll [14] had proposed a type of non-Newtonian fluid called second grade fluid. It is also one kind of viscoelastic fluid. Generally, it can be found in polymer fluid where the fluid exhibits both the viscous and elastic characteristics. In the last few years, a lot of work has been done on second grade fluid flow and the interesting works can be found in [15-23]. Few researchers have intended to study the non-coaxial rotation in the second grade fluid due to the great important in industrial applications. Hayat [24] considered the flow of a second grade fluid bounded by a non-torsional oscillating porous disk which rotates non-coaxially with a fluid at infinity. Further, Hayat [25] analytically studied the unsteady MHD second grade fluid due to eccentric rotation of a porous oscillating disk and a fluid at infinity. The exact solutions of unsteady mixed convection flow on MHD non-coaxial rotation of second grade fluid in a porous medium has been determined by Mohamad [26] by mean of Laplace transform method.

In mathematical analysis, the problems of Newtonian fluid are simpler compare to non-Newtonian fluid problems. It is due to the fact that the mathematical systems of Newtonian fluid are not as much complicated and their solutions are convenient. The problems of non-Newtonian fluid on the other hand are very complicated due to the additional non-Newtonian term in the constitutive equation. This difficulty further increases when the non-Newtonian fluid is incorporated in other physical phenomenon such as heat and mass transfer or known as double diffusion. To the best of the author's knowledge, no attempt has been made to discuss the MHD second grade fluid flow due to non-coaxial rotations of fluid at infinity and a disk with the effect of heat and mass transfer in a porous medium. In the present communication, such an attempt was given. The combined effects of double diffusion and porosity on the MHD second grade fluid flow were discussed. Laplace transform method was applied to obtain an exact solution of the governing equations. The influence of second grade parameter, magnetic field, heat and mass transfer and porosity on the flow were graphically presented and analysed.

## 2. Mathematical Modelling

Consider unsteady incompressible electrically conducting second grade fluid which embedded in a porous medium and the heat transfer occurs due to free convection as presented in Fig. 1. The $x$-axis is taken in upward direction along the plate and the $z$-axis is taken normal to the plane of the plate. The axes of rotation for both plate and fluid are assumed to be in the plane $x = 0$. A uniform transverse magnetic field of strength $B_0$ is applied parallel to the axis of rotation. It is assumed that induced magnetic field, the external electric field and the electric field due to polarization of charges are negligible. Initially, at $t = 0$ the disk and fluid at infinity are rotating about $z$'-axis in the common angular velocity $\Omega$ with constant temperature $T_\infty$ and constant concentration $C_\infty$. After time $t > 0$, the disk suddenly starts to oscillate $\omega$ in its own plan and the fluid rotates about $z$-axis with uniform angular velocity $\Omega$ while the fluid at infinity continues to rotate about $z$'-axis with the same angular velocity. Meanwhile, the temperature

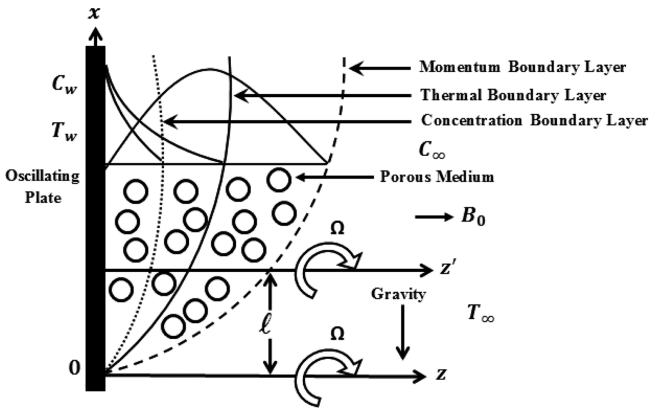


**Fig. 1.** Schematic diagram of MHD non-coaxial rotation past an oscillating vertical plate in a porous medium with heat and mass transfer effects.

of the disk is raised to constant temperature $T_w$ and constant temperature $C_w$. Here, the distance between axes of rotation is equal to $\ell$. Therefore, the initial and the boundary conditions can be written in the following form [9, 11-13]

$$\begin{aligned} u(z,0) &= -\Omega(y-\ell), \quad v(z,0) = \Omega x, \\ w(z,0) &= 0, \quad \forall z > 0, \\ u(0,t) &= -\Omega y + UH(t)\cos(\omega t) \\ &\text{or} \\ u(0,t) &= -\Omega y + U\sin(\omega t), \\ v(0,t) &= \Omega x, \quad w(0,t) = 0; \quad \forall t > 0, \\ u(\infty,t) &= -\Omega(y-\ell), \quad v(\infty,t) = \Omega x, \\ w(\infty,t) &= 0; \quad \forall t > 0, \end{aligned} \tag{1}$$

where $u$, $v$ and $w$ are respectively the velocity components along $x$, $y$ and $z$-directions. The initial and boundary conditions given by Eq. (1) suggest that the components $u$, $v$ and $w$ of the velocity can be written in the following form [9, 11-13]

$$\begin{aligned} u(z,t) &= -\Omega y + f(z,t), \; v(z,t) = \Omega x + g(z,t), \\ w(z,t) &= h(z,t), \end{aligned} \tag{2}$$

where $f(z,t)$, $g(z,t)$ and $h(z,t)$ are unknown functions. The unsteady motion of the incompressible second grade fluid subjected to Eq. (2) in Cartesian coordinates system is governed by the continuity [24, 25], Navier-Stokes [24, 25] and body force [12, 13, 24, 25] equations can be written a

$$\begin{aligned} &\left(1+\frac{\upsilon\phi\alpha_1}{\mu k_1}\right)\frac{\partial F}{\partial t} + \Omega i(F-\Omega\ell) = \\ &\left(\upsilon - \frac{\alpha_1 i\Omega}{\rho}\right)\frac{\partial^2 F}{\partial z^2} + \frac{\alpha_1}{\rho}\frac{\partial^3 F}{\partial z^2 \partial t} - \frac{\sigma B_0^2}{\rho}(F-\Omega\ell) - \\ &\frac{\upsilon\phi}{k_1}(F-\Omega\ell) + g_x\beta_T(T-T_\infty) + g_x\beta_C(C-C_\infty). \end{aligned} \tag{3}$$

From equation (3), it has the functions of temperature $T(z,t)$ and concentration $C(z,t)$ on the right hand side . Hence, introduced the energy and mass equations as follow [12, 12, 20, 21]

$$\frac{\partial T}{\partial t} = \frac{k}{\rho C_p}\frac{\partial^2 T}{\partial z^2} \tag{4}$$

and

$$\frac{\partial C}{\partial t} = D\frac{\partial^2 C}{\partial z^2} \tag{5}$$

where $\upsilon$ is the kinematic viscosity, $\phi$ is the porosity, $\alpha_1$ is material moduli commonly referred to as the normal stress moduli, $\mu$ is the dynamic viscosity, $k_1$ is the permeability of the porous medium, $F = F(z,t) = f(z,t) + ig(z,t)$ is a complex velocity [12, 13, 20, 21, 24-26], $f(z,t)$ is a primary velocity, $i$ is an unit vector in the vertical flow direction, $g(z,t)$ is a secondary velocity, $\rho$ is the density of fluid, $\sigma$ is an electrical conductivity, $g_x$ is an acceleration due to the gravity, $\beta_T$ is the volumetric coefficient of thermal expansion for temperature, $\beta_C$ is the volumetric coefficient of mass transfer, $k$ is the thermal conductivity, $C_p$ is the specific heat capacity and $D$ is the mass diffusivity. The conditions of Eq. (1) subjected to Eq. (2) and complex velocity are reduced as

$$\begin{aligned} F(z,0) &= \Omega\ell; \quad \forall z > 0, \\ F(0,t) &= UH(t)\cos(\omega t) \text{ or } F(0,t) = U\sin(\omega t); \; \forall t > 0, \\ F(\infty,t) &= \Omega\ell; \quad \forall t > 0, \end{aligned} \tag{6}$$

Then, conditions for energy and mass equation are introduced as

$$\begin{aligned} T(z,0) &= T_\infty; \quad \forall z > 0, \\ T(0,t) &= T_w; \quad \forall t > 0, \\ T(\infty,t) &= T_\infty; \quad \forall t > 0, \end{aligned} \tag{7}$$

$$\begin{aligned} C(z,0) &= C_\infty; \quad \forall z > 0, \\ C(0,t) &= C_w; \quad \forall t > 0, \\ C(\infty,t) &= C_\infty; \quad \forall t > 0, \end{aligned} \tag{8}$$

where $U$ is the amplitude of the plate oscillations, $H(t)$ is a Heaviside function, $\omega$ is a frequency of oscillation, $\sin(\omega t)$ and $\cos(\omega t)$ are trigonometric functions for sine and cosine oscillation cases. Here, the Eqs. (3) until (8) are dimensional equations which are involved SI unit. Therefore, in order to eliminate SI unit and simply these dimensional equations, we introduced the non-dimensional variables as follow

$$\begin{aligned} &F^* = \frac{F}{\Omega\ell} - 1, \; z^* = \sqrt{\frac{\Omega}{\upsilon}}z, \; t^* = \Omega t, \; \omega^* = \frac{\omega}{\Omega}, \\ &T^* = \frac{T-T_\infty}{T_w - T_\infty}, \; C^* = \frac{C-C_\infty}{C_w - C_\infty} \end{aligned} \tag{9}$$

to obtain the non-dimensional equations. Then, substitute the non-dimensional variables (9) into Eqs. (3) until (8), obtained (dropping out the * notation):

$$n_7\frac{\partial F}{\partial t} + n_8 F = m_1\frac{\partial^2 F}{\partial z^2} + \alpha\frac{\partial^3 F}{\partial z^2 \partial t} + GrT + GmC, \tag{10}$$

$$\frac{\partial T}{\partial t} = \frac{1}{\mathrm{Pr}}\frac{\partial^2 T}{\partial z^2}, \tag{11}$$

$$\frac{\partial C}{\partial t} = \frac{1}{Sc}\frac{\partial^2 C}{\partial z^2}, \tag{12}$$

with initial and boundary conditions

$$\begin{aligned} &F(z,0)=0, \quad \forall z>0,\\ &F(0,t)=-1+U_0H(t)\cos(\omega t) \text{ or}\\ &F(0,t)=-1+U_0\sin(\omega t); \quad \forall t>0,\\ &F(\infty,t)=0; \quad \forall t>0 \end{aligned} \tag{13}$$

$$\begin{aligned} &T(z,0)=0; \quad \forall z>0,\\ &T(0,t)=1; \quad \forall t>0,\\ &T(\infty,t)=0; \quad \forall t>0, \end{aligned} \tag{14}$$

$$\begin{aligned} &C(z,0)=0; \quad \forall z>0,\\ &C(0,t)=1; \quad \forall t>0,\\ &C(\infty,t)=0; \quad \forall t>0. \end{aligned} \tag{15}$$

From this non-dimensional process will be obtained the important parameters such as

$$\begin{aligned} &n_7=1+\frac{\alpha}{K}, \quad n_8=i+M^2+\frac{1}{K}, \quad m_1=1-\alpha i,\\ &\alpha=\frac{\alpha_1\Omega}{\rho\upsilon}, \quad \frac{1}{K}=\frac{\upsilon\phi}{\Omega k}, \quad M=\frac{\sigma B_0^2}{\rho\Omega},\\ &Gr=\frac{g_x\beta_T(T_w-T_\infty)}{\Omega^2\ell}, \quad Gm=\frac{g_x\beta_C(C_w-C_\infty)}{\Omega^2\ell},\\ &\Pr=\frac{\mu c_p}{k}, \quad Sc=\frac{\upsilon}{D}, \quad U_0=\frac{U}{\Omega\ell}. \end{aligned} \tag{16}$$

where $\alpha$ is the second grade parameter, $K$ is the porosity parameter, $M$ is the magnetic parameter, $Gr$ is the Grashof Number, $Gm$ is the modified Grashof Number, Pr is the Prandtl Number, $Sc$ is the Schmidt Number and $U_0$ is the non-dimensional parameter of amplitude of the plate oscillations. As mentioned in introduction, the solution of this problem will be obtained by using Laplace transform method. Then, apply this Laplace transform to Eqs. (10) until (15) subjected to initial conditions (13) until (15), obtained transform of momentum, energy and mass equations as followed

$$\frac{d^2\bar{F}}{dz^2}-\left(\frac{n_7q+n_8}{\alpha q+m_1}\right)\bar{F}=-\frac{Gr}{m_1+\alpha q}\bar{T}-\frac{Gm}{m_1+\alpha q}\bar{C}, \tag{17}$$

$$\frac{d^2\bar{T}}{dz^2}-q\Pr\bar{T}=0, \tag{18}$$

$$\frac{d^2\bar{C}}{dz^2}-qSc\bar{C}=0, \tag{19}$$

and transform of boundary condition are

$$\begin{aligned} &\bar{F}(0,q)=-\frac{1}{q}+U_0\frac{q}{q^2+\omega^2} \text{ or } \bar{F}(0,q)=-\frac{1}{q}+U_0\frac{\omega}{q^2+\omega^2},\\ &\bar{F}(\infty,q)=0, \end{aligned} \tag{20}$$

$$\bar{C}(0,q)=\frac{1}{q}, \quad \bar{C}(\infty,q)=0, \tag{21}$$

$$\bar{T}(0,q)=\frac{1}{q}, \quad \bar{T}(\infty,q)=0, \tag{22}$$

where $\bar{F}=\bar{F}(z,q)$, $\bar{T}=\bar{T}(z,q)$, $\bar{C}=\bar{C}(z,q)$, and $q$ is the domain of Laplace transformation parameter. In order to solve Eq. (17), first we need to obtain the solution of Eqs. (18) and (19) by using the homogenous characteristics equation subjected the boundary conditions (21) and (22). Here, it can be written as

$$\bar{T}=\frac{1}{q}\exp(-z\sqrt{q\Pr}) \tag{23}$$

and

$$\bar{C}=\frac{1}{q}\exp(-z\sqrt{qSc}). \tag{24}$$

After that, substitute Eqs. (23) and (24) into Eq. (17), we obtained

$$\begin{aligned} &\frac{d^2\bar{F}}{dz^2}-\left(\frac{n_7q+n_8}{\alpha q+m_1}\right)\bar{F}=-\frac{Gr}{m_1+\alpha q}\cdot\frac{1}{q}\exp\left(-z\sqrt{q\Pr}\right)\\ &-\frac{Gm}{m_1+\alpha q}\cdot\frac{1}{q}\exp\left(-z\sqrt{qSc}\right), \end{aligned} \tag{25}$$

and solve this Eq. (25) by using non-homogenous characteristics equation where can be written as

$$\bar{F}(z,q)=\bar{F}_h(z,q)+\bar{F}_{p1}(z,q)+\bar{F}_{p2}(z,q) \tag{26}$$

which is

$$\begin{aligned} \bar{F}_h(z,q)=&c_1\exp\left(-z\sqrt{n_9}\sqrt{\frac{q+n_{10}}{q+m_4}}\right)\\ &+c_2\exp\left(z\sqrt{n_9}\sqrt{\frac{q+n_{10}}{q+m_4}}\right), \end{aligned} \tag{27}$$

$$\bar{F}_{p1}(z,q)=-\frac{Gr}{\alpha\Pr}\cdot\frac{1}{q[q^2+n_{12}q-n_{13}]}\exp(-z\sqrt{q\Pr}) \tag{28}$$

and

$$\bar{F}_{p2}(z,q)=-\frac{Gm}{\alpha Sc}\cdot\frac{1}{q[q^2+N_1q-N_2]}\exp(-z\sqrt{qSc}). \tag{29}$$

To find the values of constant $c_1$ and $c_2$ in Eq. (27), the boundary condition (20) need to be used subjected to Eqs. (26), (28), (29) and obtained as

$$\begin{aligned} &\bar{F}(z,q)=\left[U_0\frac{q}{q^2+\omega^2}-\frac{1}{q}\right]\exp\left(-z\sqrt{n_9}\sqrt{\frac{q+n_{10}}{q+m_4}}\right)+\\ &\frac{Gr}{\alpha\Pr}\cdot\frac{1}{q[q^2+n_{12}q-n_{13}]}\left[\exp\left(-z\sqrt{n_9}\sqrt{\frac{q+n_{10}}{q+m_4}}\right)-\exp(-z\sqrt{q\Pr})\right]+\\ &\frac{Gm}{\alpha Sc}\cdot\frac{1}{q[q^2+N_1q-N_2]}\left[\exp\left(-z\sqrt{n_9}\sqrt{\frac{q+n_{10}}{q+m_4}}\right)-\exp(-z\sqrt{q\Pr})\right]. \end{aligned} \tag{30}$$

$$\bar{F}(z,q)=\left[U_0\frac{\omega}{q^2+\omega^2}-\frac{1}{q}\right]\exp\left(-z\sqrt{n_9}\sqrt{\frac{q+n_{10}}{q+m_4}}\right)+$$
$$\frac{Gr}{\alpha\,\mathrm{Pr}}\cdot\frac{1}{q[q^2+n_{12}q-n_{13}]}\left[\exp\left(-z\sqrt{n_9}\sqrt{\frac{q+n_{10}}{q+m_4}}\right)-\exp(-z\sqrt{q\,\mathrm{Pr}})\right]+$$
$$\frac{Gm}{\alpha Sc}\cdot\frac{1}{q[q^2+N_1q-N_2]}\left[\exp\left(-z\sqrt{n_9}\sqrt{\frac{q+n_{10}}{q+m_4}}\right)-\exp(-z\sqrt{q\,\mathrm{Pr}})\right]. \tag{31}$$

where Eqs. (30) and (31) are the functions of cosine and sine oscillation cases. Then the solution of the differential equation as a function of $t$ will be found by taking inverse Laplace transform of Eqs. (23), (24), (30) and (31). Here, we received as

$$T(z,t)=erfc\left(\frac{z\sqrt{\mathrm{Pr}}}{2\sqrt{t}}\right), \tag{32}$$

$$C(z,t)=erfc\left(\frac{z\sqrt{Sc}}{2\sqrt{t}}\right), \tag{33}$$

$$F(z,t)=[U_0H(t)\cos(\omega t)-1]\exp(-z\sqrt{n_9})+$$
$$zn_{15}\int_0^t\int_0^\infty\frac{1}{u\sqrt{s}}H(t-s)\cos(\omega t-\omega s)$$
$$\exp\left(-\frac{z^2n_9}{4u}-m_4s-u\right)I_1(2\sqrt{n_{14}us})duds-$$
$$zn_{16}\int_0^t\int_0^\infty\frac{1}{u\sqrt{s}}\exp\left(-\frac{z^2n_9}{4u}-m_4s-u\right)I_1(2\sqrt{n_{14}us})duds+$$
$$\frac{m_8}{n_{18}}\int_0^t\sinh(n_{18}(t-r))\exp(-n_{17}(t-r)-z\sqrt{n_9})dr+$$
$$zn_{19}\int_0^t\int_0^r\int_0^\infty\frac{1}{u\sqrt{s}}\sinh(n_{18}(t-r))\exp\left(-\frac{z^2n_9}{4u}-m_4s-u-n_{17}(t-r)\right)$$
$$I_1(2\sqrt{n_{14}us})dudsdr-$$
$$\frac{m_8}{n_{18}}\int_0^t\sinh(n_{18}(t-r))\exp(-n_{17}(t-r))erfc\left(\frac{1}{2}\sqrt{\frac{\mathrm{Pr}}{r}}z\right)dr+$$
$$\frac{N_3}{N_5}\int_0^t\sinh(N_5(t-r))\exp(-N_4(t-r)-z\sqrt{n_9})dr+$$
$$zN_6\int_0^t\int_0^r\int_0^\infty\frac{1}{u\sqrt{s}}\sinh(N_5(t-r))\exp\left(-\frac{z^2n_9}{4u}-m_4s-u-N_4(t-r)\right)$$
$$I_1(2\sqrt{n_{14}us})dudsdr-$$
$$\frac{N_3}{N_5}\int_0^t\sinh(N_5(t-r))\exp(-N_4(t-r))erfc\left(\frac{1}{2}\sqrt{\frac{Sc}{r}}z\right)dr, \tag{34}$$

$$F(z,t)=[U_0\sin(\omega t)-1]\exp(-z\sqrt{n_9})+$$
$$zn_{15}\int_0^t\int_0^\infty\frac{1}{u\sqrt{s}}H(t-s)\sin(\omega t-\omega s)$$
$$\exp\left(-\frac{z^2n_9}{4u}-m_4s-u\right)I_1(2\sqrt{n_{14}us})duds-$$
$$zn_{16}\int_0^t\int_0^\infty\frac{1}{u\sqrt{s}}\exp\left(-\frac{z^2n_9}{4u}-m_4s-u\right)I_1(2\sqrt{n_{14}us})duds+$$
$$\frac{m_8}{n_{18}}\int_0^t\sinh(n_{18}(t-r))\exp(-n_{17}(t-r)-z\sqrt{n_9})dr+$$
$$zn_{19}\int_0^t\int_0^r\int_0^\infty\frac{1}{u\sqrt{s}}\sinh(n_{18}(t-r))\exp\left(-\frac{z^2n_9}{4u}-m_4s-u-n_{17}(t-r)\right)$$
$$I_1(2\sqrt{n_{14}us})dudsdr-$$
$$\frac{m_8}{n_{18}}\int_0^t\sinh(n_{18}(t-r))\exp(-n_{17}(t-r))erfc\left(\frac{1}{2}\sqrt{\frac{\mathrm{Pr}}{r}}z\right)dr+$$
$$\frac{N_3}{N_5}\int_0^t\sinh(N_5(t-r))\exp(-N_4(t-r)-z\sqrt{n_9})dr+$$
$$zN_6\int_0^t\int_0^r\int_0^\infty\frac{1}{u\sqrt{s}}\sinh(N_5(t-r))\exp\left(-\frac{z^2n_9}{4u}-m_4s-u-N_4(t-r)\right)$$
$$I_1(2\sqrt{n_{14}us})dudsdr-$$
$$\frac{N_3}{N_5}\int_0^t\sinh(N_5(t-r))\exp(-N_4(t-r))erfc\left(\frac{1}{2}\sqrt{\frac{Sc}{r}}z\right)dr, \tag{35}$$

where Eq. (32), Eq. (33), Eq. (34) and Eq. (35) are final solutions for energy (temperature profile), mass (concentration profile) and momentum (velocity profile) equations for cosine and sine oscillation cases. Hence, the Nusselt number, Sherwood number and skin friction of solutions (32), (33), Eq. (34) and (35) can be expressed as:

$$Nu=-\left[\frac{\partial T}{\partial z}\right]_{z=0}, \tag{36}$$

$$Sh=-\left[\frac{\partial C}{\partial z}\right]_{z=0}, \tag{37}$$

$$\tau=-\left[\left(m_1+\alpha\frac{\partial}{\partial t}\right)\frac{\partial F}{\partial z}\right]_{z=0}, \tag{38}$$

Therefore, solution of Eq. (36), Eq. (37) and Eq. (38) in view of Eq. (32), Eq. (33), Eq. (34) and Eq. (35) can be obtained as

$$Nu=\sqrt{\frac{\mathrm{Pr}}{\pi t}} \tag{39}$$

$$Sh=\sqrt{\frac{Sc}{\pi t}} \tag{40}$$

$$\tau_c=\left(m_1-\alpha\frac{\partial}{\partial t}\right)\tau_1(t) \tag{41}$$

and

$$\tau_s=\left(m_1-\alpha\frac{\partial}{\partial t}\right)\tau_2(t) \tag{42}$$

where

$$\tau_1(t)=\sqrt{n_9}\,(1-U_0\cos(\omega t))+ n_{15}\int_0^t\int_0^\infty \frac{1}{u\sqrt{s}}\cos(\omega t-\omega s)\exp(-m_4 s-u)\,I_1(2\sqrt{n_{14}us})\,duds- n_{16}\int_0^t\int_0^\infty \frac{1}{u\sqrt{s}}\exp(-m_4 s-u)\,I_1(2\sqrt{n_{14}us})\,duds+ n_{20}\int_0^t\int_0^r\int_0^\infty \frac{\sinh(n_{18}(t-r))}{\exp(-m_4 s-u-n_{17}(t-r))\,I_1(2\sqrt{n_{14}us})}\,\frac{1}{u\sqrt{s}}\,dudsdr+ n_{19}\sqrt{\frac{\mathrm{Pr}}{\pi}}\int_0^t\frac{1}{\sqrt{r}}\sinh(n_{18}(t-r))\exp(-n_{17}(t-r))dr- n_{19}\sqrt{n_9}\int_0^t\sinh(n_{18}(t-r))\exp(-n_{17}(t-r))dr+ N_7\int_0^t\int_0^r\int_0^\infty \frac{\sinh(N_5(t-r))}{\exp(-m_4 s-u-N_4(t-r))\,I_1(2\sqrt{n_{14}us})}\,\frac{1}{u\sqrt{s}}\,dudsdr+ N_6\sqrt{\frac{Sc}{\pi}}\int_0^t\frac{1}{\sqrt{r}}\sinh(N_5(t-r))\exp(-N_4(t-r))dr- N_6\sqrt{n_9}\int_0^t\sinh(N_5(t-r))\exp(-N_4(t-r))dr \quad (43)$$

and

$$\tau_2(t)=\sqrt{n_9}\,(1-U_0\sin(\omega t))+ n_{15}\int_0^t\int_0^\infty \frac{1}{u\sqrt{s}}\sin(\omega t-\omega s)\exp(-m_4 s-u)\,I_1(2\sqrt{n_{14}us})\,duds- n_{16}\int_0^t\int_0^\infty \frac{1}{u\sqrt{s}}\exp(-m_4 s-u)\,I_1(2\sqrt{n_{14}us})\,duds+ n_{20}\int_0^t\int_0^r\int_0^\infty \frac{\sinh(n_{18}(t-r))}{\exp(-m_4 s-u-n_{17}(t-r))\,I_1(2\sqrt{n_{14}us})}\,\frac{1}{u\sqrt{s}}\,dudsdr+ n_{19}\sqrt{\frac{\mathrm{Pr}}{\pi}}\int_0^t\frac{1}{\sqrt{r}}\sinh(n_{18}(t-r))\exp(-n_{17}(t-r))dr- n_{19}\sqrt{n_9}\int_0^t\sinh(n_{18}(t-r))\exp(-n_{17}(t-r))dr+ N_7\int_0^t\int_0^r\int_0^\infty \frac{\sinh(N_5(t-r))}{\exp(-m_4 s-u-N_4(t-r))\,I_1(2\sqrt{n_{14}us})}\,\frac{1}{u\sqrt{s}}\,dudsdr+ N_6\sqrt{\frac{Sc}{\pi}}\int_0^t\frac{1}{\sqrt{r}}\sinh(N_5(t-r))\exp(-N_4(t-r))dr- N_6\sqrt{n_9}\int_0^t\sinh(N_5(t-r))\exp(-N_4(t-r))dr. \quad (44)$$

Here, $m_4=\frac{m_1}{\alpha}$, $m_8=\frac{Gr}{\alpha\,Pr}$, $n_9=\frac{n_7}{\alpha}$, $n_{10}=\frac{n_8}{n_7}$, $n_{11}=n_9n_{10}$, $n_{12}=\frac{m_4\,Pr-n_9}{Pr}$, $n_{13}=\frac{n_{11}}{Pr}$, $n_{14}=m_4-n_{10}$, $n_{15}=\frac{U_0\sqrt{n_9n_{14}}}{2\sqrt{\pi}}$, $n_{16}=\frac{\sqrt{n_9n_{14}}}{2\sqrt{\pi}}$, $n_{17}=\frac{n_{12}}{2}$, $n_{18}=\sqrt{\frac{n_{12}^2-4n_{13}}{4}}$, $n_{19}=\frac{m_8}{n_{18}}$, $n_{20}=\frac{m_8\sqrt{n_9n_{14}}}{2n_{18}\sqrt{\pi}}$, $N_1=\frac{m_4Sc-n_9}{Sc}$, $N_2=\frac{n_{11}}{Sc}$, $N_3=\frac{Gm}{\alpha Sc}$, $N_4=\frac{N_1}{2}$, $N_5=\sqrt{\frac{N_1^2+4N_2}{4}}$, $N_6=\frac{N_3}{N_5}$ and $N_7=\frac{N_6\sqrt{n_9n_{14}}}{2\sqrt{\pi}}$.

## 3. Validation

In order to check the accuracy of the results as shown in Fig. 2, the validation process has been done by comparing the cosine and sine oscillations with those of Guria [10]. By allowing the parameters of slip condition, suction $S$ and magnetic $M$ to be equal to zero in Eq. (32) of Guria [10] and it is found that the result was identical to Eqs. (34-35) when parameters $K\to\infty$, $M=Gr=Gm=0$ and $\alpha=\mathrm{Pr}=\mathrm{Sc}\to 0$. These solutions are called

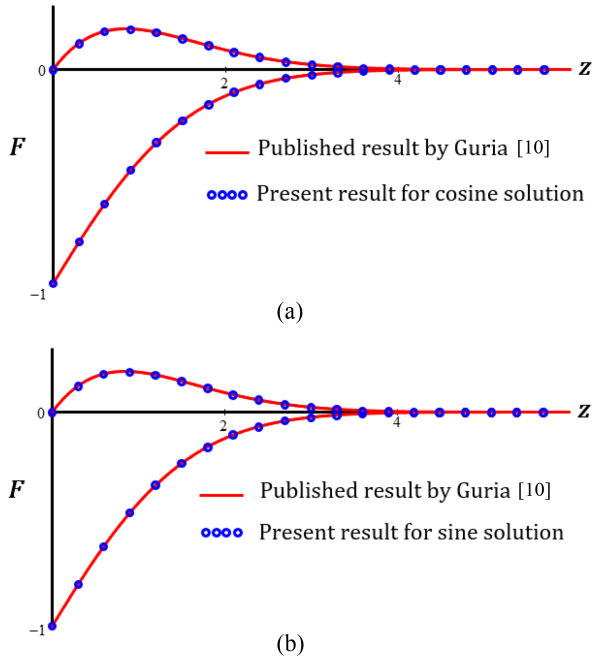


**Fig. 2.** (Color online) Comparison of velocity profile in Eqs. (34-35) with Eq. (32) of Guria [10] for (a) cosine solution and (b) sine solution.

**Table 1.** Comparison of the primary velocity results $f(z,t)$ (34) for cosine case.

| $z$ | Exact solution | Numerical solution (Ref. [27, 28]) | \|Error\| |
|---|---|---|---|
| 0 | 0.500 | 0.499 | 0.001 |
| 1 | 1.297 | 1.296 | 0.001 |
| 2 | 0.717 | 0.717 | 0.000 |
| 3 | 0.276 | 0.276 | 0.000 |
| 4 | 0.085 | 0.084 | 0.001 |

[a]Ref. [27, 28]

**Table 2.** Comparison of the comparison velocity results $g(z,t)$ (34) for cosine case.

| $z$ | Exact solution | Numerical solution (Ref. [27, 28]) | \|Error\| |
|---|---|---|---|
| 0 | 0.500 | 0.499 | 0.001 |
| 1 | 0.272 | 0.271 | 0.001 |
| 2 | 0.303 | 0.302 | 0.001 |
| 3 | 0.194 | 0.193 | 0.001 |
| 4 | 0.096 | 0.096 | 0.000 |

[a]Ref. [27, 28]

**Table 3.** Comparison of the primary velocity results $f(z,t)$ (35) for sine case.

| $z$ | Exact solution | Numerical solution (Ref. [27, 28]) | \|Error\| |
|---|---|---|---|
| 0 | 1.598 | 1.598 | 0.000 |
| 1 | 1.544 | 1.544 | 0.000 |
| 2 | 0.805 | 0.805 | 0.000 |
| 3 | 0.324 | 0.324 | 0.000 |
| 4 | 0.112 | 0.112 | 0.000 |

[a]Ref. [27, 28]

**Table 4.** Comparison of the secondary velocity results $g(z,t)$ (35) for sine case.

| $z$ | Exact solution | Numerical solution (Ref. [27,28]) | \|Error\| |
|---|---|---|---|
| 0 | 0.000 | 0.000 | 0.000 |
| 1 | 1.098 | 1.098 | 0.000 |
| 2 | 0.164 | 0.164 | 0.000 |
| 3 | 0118 | 0118 | 0.000 |
| 4 | 0.063 | 0.063 | 0.000 |

limiting cases. In addition, the accuracy of the results is also verified by comparing with numerical results as shown in Tables 1 to 4. Eqs. (34-35) have been solved numerically by using Gaver–Stehfest algorithm [27, 28] for inverse Laplace transform. These tables showed that results of primary, $f(z,t)$ and secondary $g(z,t)$ velocities for the cosine and sine cases from exact (Eqs. (34-35)) and numerical solutions are found to be in good agreement.

## 4. Results and Discussion

This chapter has discussed the formulation of the exact solutions for unsteady MHD free convection flow of a non–coaxial rotation second grade fluid in porous medium of Eqs. (34, 35) in double diffusion, by using the Laplace transform method. Accordingly, the problems over an oscillating disk for the case of sine and cosine have been discussed. Graphical results have also been prepared to

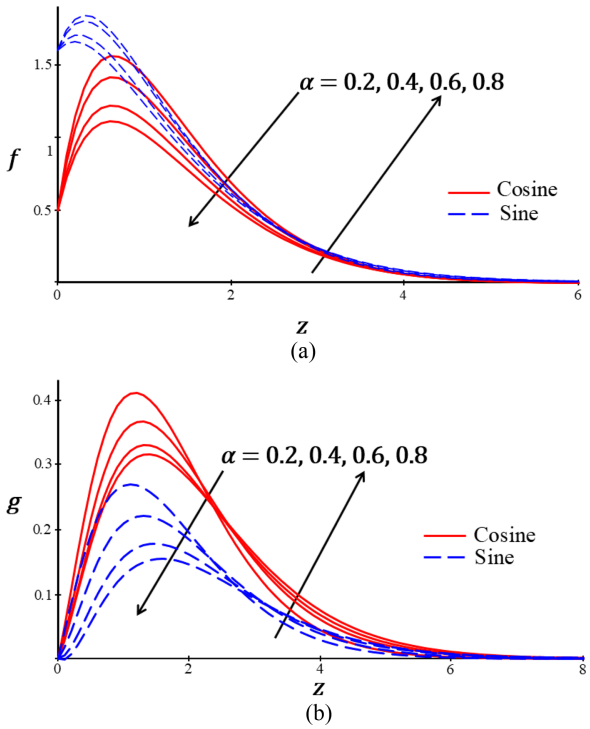


**Fig. 3.** (Color online) Velocity profiles for different values of $\alpha$ with $Gr$ = 5.00, $Gm$ = 5.00, Pr = 1.00, $Sc$ = 0.62, $M$ = 0.20, $K$ = 2.00, $t$ = 1.00, $U_0$ = 3.00 and $\omega$ = $\pi$/3 for (a) Primary velocity and (b) Secondary velocity.

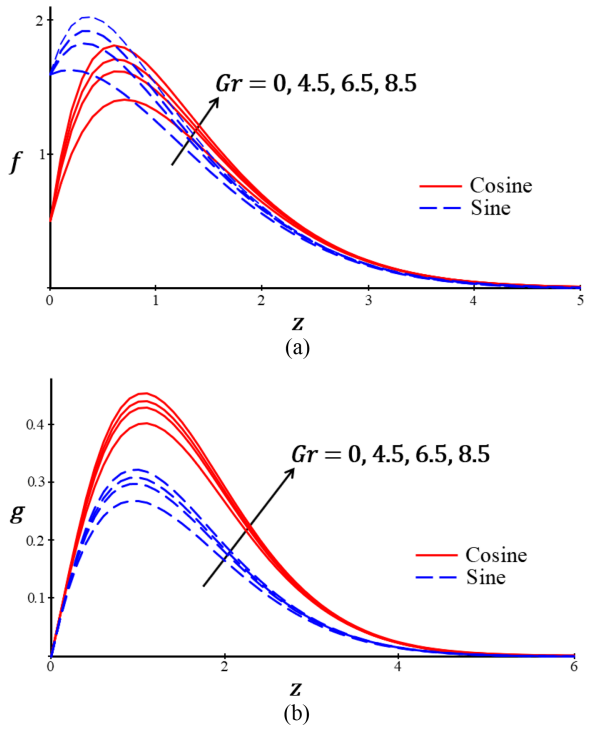


**Fig. 4.** (Color online) Velocity profiles for different values of $Gr$ with $\alpha$ = 3.00, $Gm$ = 5.00, Pr = 1.00, $Sc$ = 0.62, $M$ = 0.20, $K$ = 2.00, $t$ = 1.00, $U_0$ = 3.00 and $\omega$ = $\pi$/3 for (a) Primary velocity and (b) Secondary velocity.

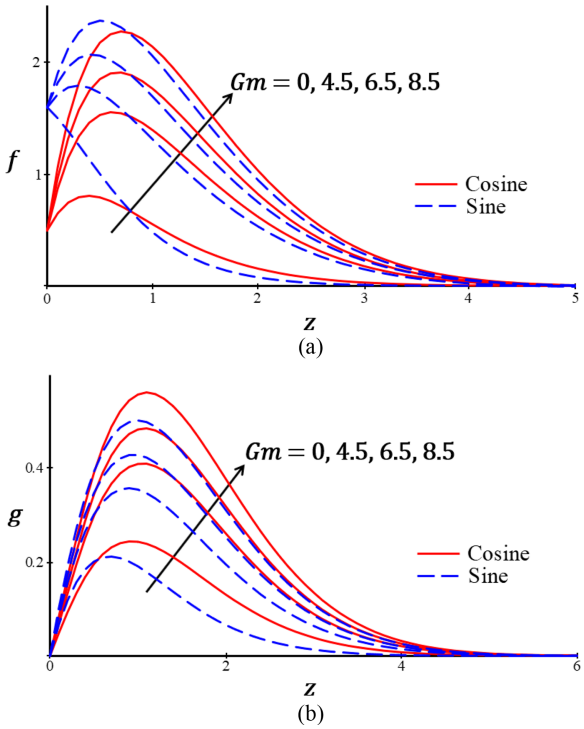


**Fig. 5.** (Color online) Velocity profiles for different values of $Gm$ with $\alpha = 3.00$, $Gr = 5.00$, Pr = 1.00, $Sc = 0.62$, $M = 0.20$, $K = 2.00$, $t = 1.00$, $U_0 = 3.00$ and $\omega = \pi/3$ for (a) Primary velocity and (b) Secondary velocity.

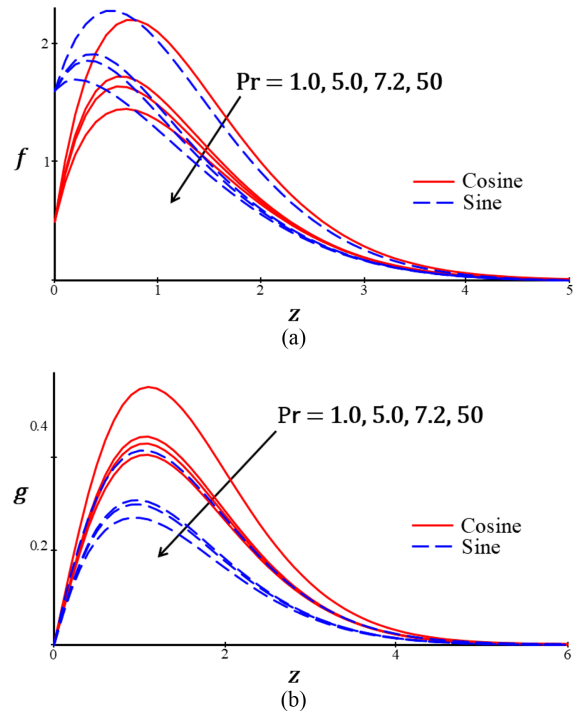


**Fig. 6.** (Color online) Velocity profiles for different values of Pr with $\alpha = 3.00$, $Gr = 5.00$, $Gm = 5.00$, $Sc = 0.62$, $M = 0.20$, $K = 2.00$, $t = 1.00$, $U_0 = 3.00$ and $\omega = \pi/3$ for (a) Primary velocity and (b) Secondary velocity.

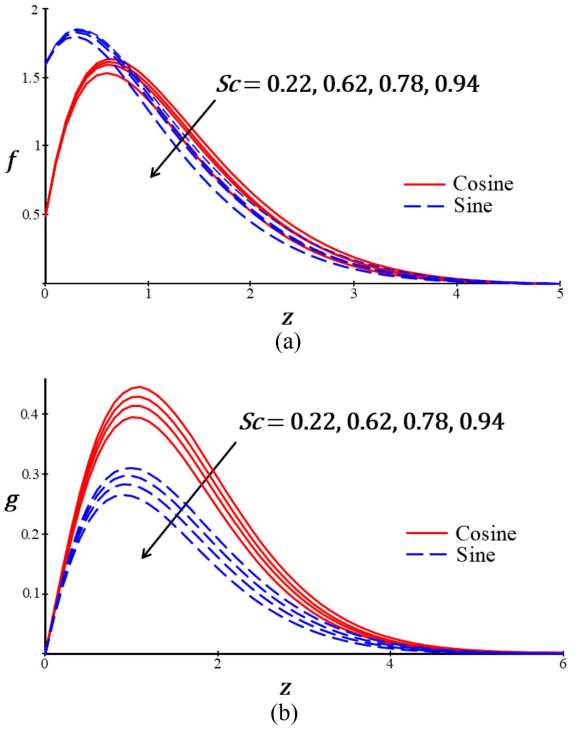


**Fig. 7.** (Color online) Velocity profiles for different values of $Sc$ with $\alpha = 3.00$, $Gr = 5.00$, $Gm = 5.00$, Pr = 1.00, $M = 0.20$, $K = 2.00$, $t = 1.00$, $U_0 = 3.00$ and $\omega = \pi/3$ for (a) Primary velocity and (b) Secondary velocity.

support the exact solutions for the effects of $\alpha$, $Gr$, $Gm$, Pr, $Sc$, $M$, $K$, $t$, $U_0$ and $\omega t$ as shown in Figs. 3 to 14. The velocity profiles have been divided into two parts, which are primary $f(z,t)$ and secondary $g(z,t)$ velocities. Figure 3 illustrates the effects of the second grade parameter $\alpha$ on the primary velocity and secondary velocity, respectively. These figures show that the primary velocity initially decreases and then increases when $\alpha$ is increased. Similar behaviour has been observed for the relationship between the secondary velocity and second grade parameter. This is due to the properties of second grade fluid as it possesses viscosity and elastic behavior. The results of velocity profiles for the influence of $Gr$ and $Gm$ are shown in Figs. 4 to 5 respectively. The velocity profiles for primary velocity or secondary velocity increase when the values of $Gr$ and $Gm$ are increased. This is because, larger values of $Gr$ and $Gm$ lead to larger buoyancy force; consequently accelerating the movement of mass particles in the fluid flow.

Figure 6 shows the behavior of the second grade fluid flows due to the influence of the Prandtl number Pr. Here, four physical values of the Pr = 1.00 (electrolyte), Pr = 5.00 (light organic fluid), Pr = 7.20 (sea water) and Pr = 50 (oil) have been chosen. It can be clearly seen from

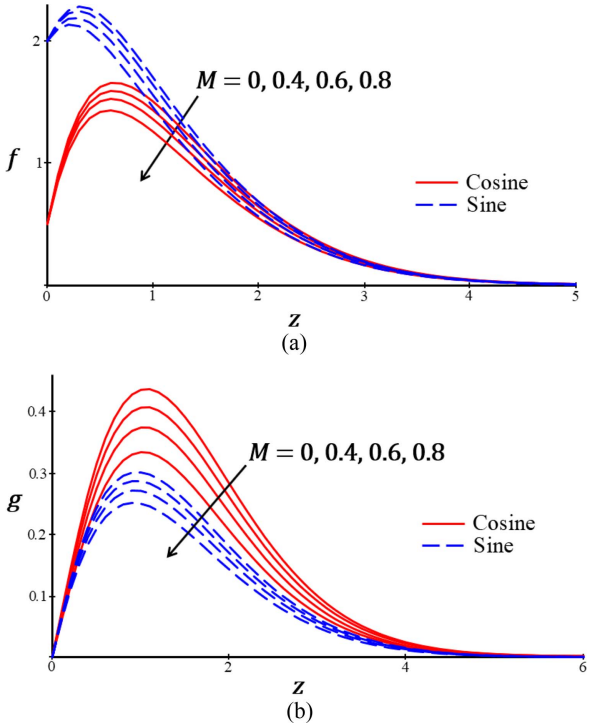


**Fig. 8.** (Color online) Velocity profiles for different values of $M$ with $\alpha = 3.00$, $Gr = 5.00$, $Gm = 5.00$, Pr = 1.00, $Sc = 0.62$, $K = 2.00$, $t = 1.00$, $U_0 = 3.00$ and $\omega = \pi/3$ for (a) Primary velocity and (b) Secondary velocity.

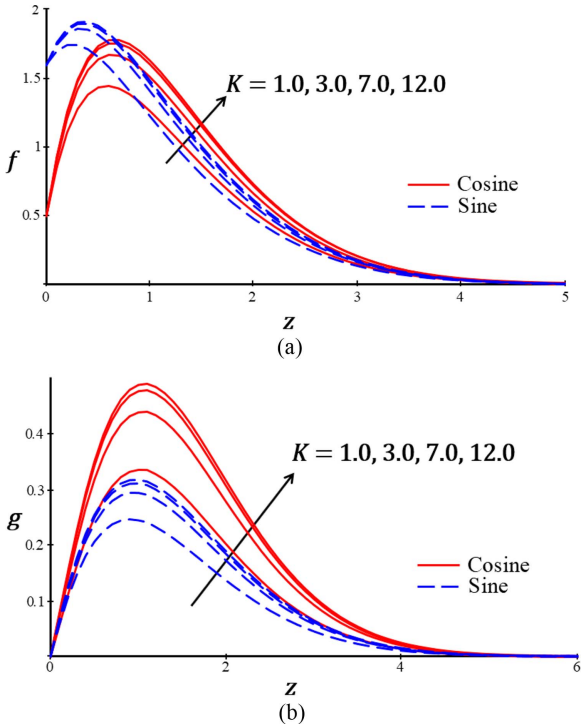


**Fig. 9.** (Color online) Velocity profiles for different values of $K$ with $\alpha = 3.00$, $Gr = 5.00$, $Gm = 5.00$, Pr = 1.00, $Sc = 0.62$, $M = 0.20$, $t = 1.00$, $U_0 = 3.00$ and $\omega = \pi/3$ for (a) Primary velocity and (b) Secondary velocity.

these figures that, velocity decreases when the values of Pr is increased. Similar phenomenon is observed for the effect of Schmidt number $Sc$ on the velocity distribution in the fluid (see Fig. 6). In this case, four different values of Schmidt number $Sc$ = 0.22; 0.62; 0.78; and 0.94 have been chosen; each physically corresponding to hydrogen, water vapour, ammonia, and carbon dioxide. Viscous force that acts on the fluid flow increases when the values of Pr and $Sc$ are increased hence reducing the movement of the second grade fluid because more energy is used against the viscous force. Noted that, the same behavior of Pr and $Sc$ is shown in temperature profile (Fig. 13) and concentration profile (Fig. 14). Figure 8 presents the effects of the magnetic parameter $M$ on the velocity profile. Either the primary velocity or the secondary velocity is reduced as the magnetic parameter is increased. In this case, the Lorentz force, which acts in opposite direction of the fluid flows, increases when the magnetic parameter is increased. Therefore, more energy is needed by the fluid to resist the frictional force (Lorentz force), thus reducing its velocity.

The drag force is reduced when porosity parameter $K$ is reduced, thus the velocity profiles increases when the porosity parameter is increased. This is due to increase

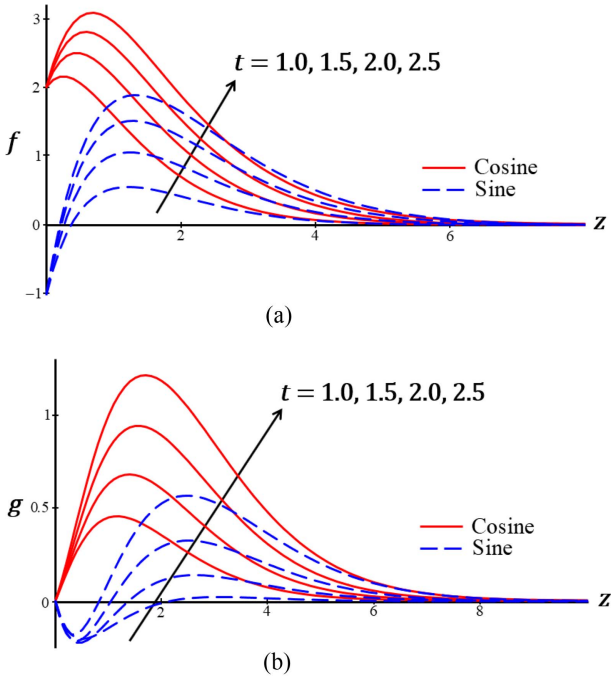


**Fig. 10.** (Color online) Velocity profiles for different values of $t$ with $\alpha = 3.00$, $Gr = 5.00$, $Gm = 5.00$, Pr = 1.00, $Sc = 0.62$, $M = 0.20$, $K = 2.00$, $U_0 = 3.00$ and $\omega = \pi/3$ for (a) Primary velocity and (b) Secondary velocity.

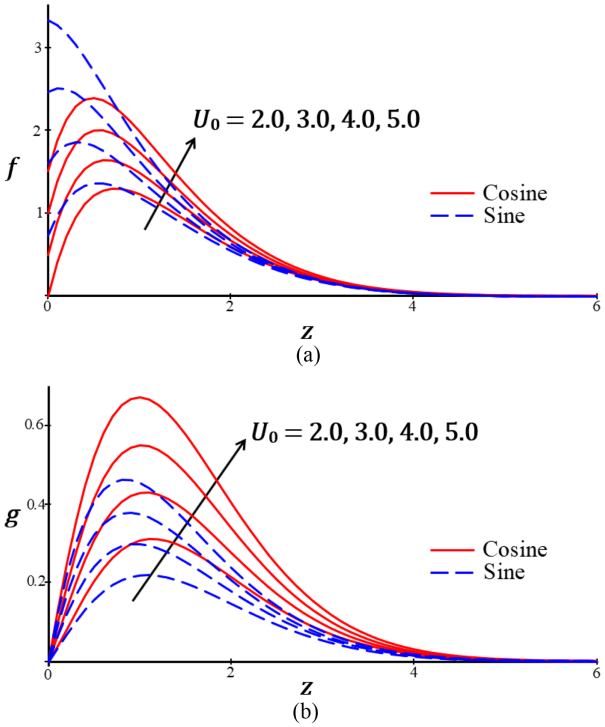


**Fig. 11.** (Color online) Velocity profiles for different values of $U_0$ with $\alpha = 3.00$, $Gr = 5.00$, $Gm = 5.00$, Pr = 1.00, $Sc = 0.62$, $M = 0.20$, $K = 2.00$, $t = 1.00$ and $\omega = \pi/3$ for (a) Primary velocity and (b) Secondary velocity.

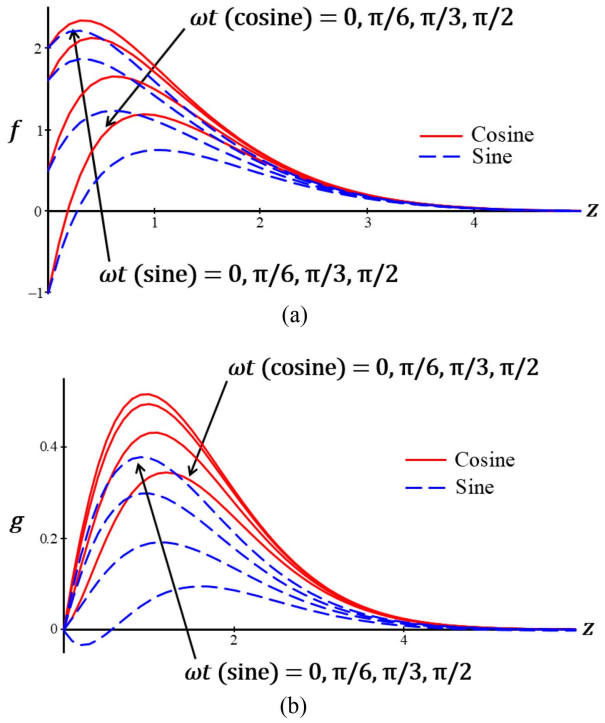


**Fig. 12.** (Color online) Velocity profiles for different values of $\omega t$ with $\alpha = 3.00$, $Gr = 5.00$, $Gm = 5.00$, Pr = 1.00, $Sc = 0.62$, $M = 0.20$, $K = 2.00$, $t = 1.00$ and $U_0 = 3.00$ for (a) Primary velocity and (b) Secondary velocity.

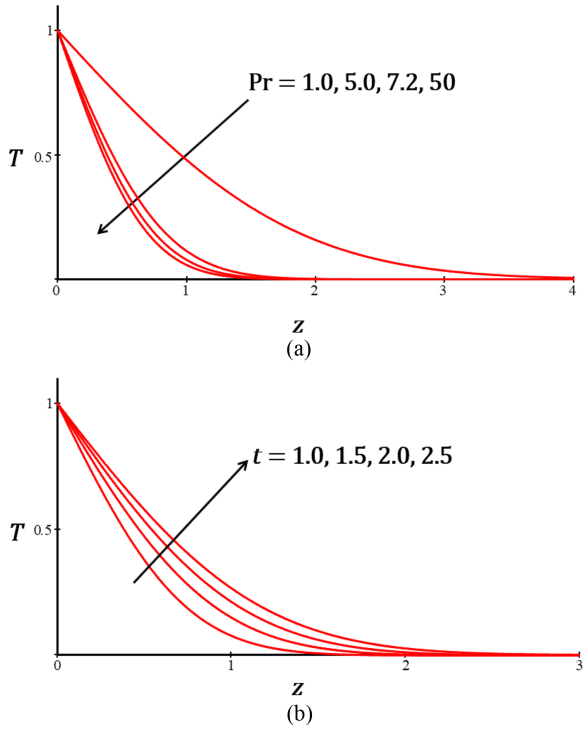


**Fig. 13.** (Color online) Temperature profiles for different values of (a) Pr with $t = 1.00$ and (b) $t$ with Pr = 1.00.

the size of the hole in porous medium that passing through the fluid flow. This behavior of the velocity profile due to the porosity parameter is presented in Fig. 9. The effects of time $t$ and parameter of amplitude of the plate oscillations $U_0$ on velocity distribution are shown in Figs. 10 to 11, respectively. It can be seen from these figures that the velocity has similar behavior when parameters $t$ and $U_0$ are increased. Both the primary velocity and secondary velocity increase when the parameters are increased. Temperature and concentration distributions for the effect of $t$ are shown in Figs. 13 to 14, respectively. Similar behavior as velocity is shown in these two profiles when parameter $t$ is increased. The influence of phase plane angle $\omega t$ on velocity profile is shown in Fig. 12. Here, the velocity decreases when the value of $\omega t$ is increased for cosine. However, opposite phenomena is observed for sine. This is due to the physical behavior of the cosine function and sine function. Furthermore, the boundary condition is satisfied by the obtained solution as seen in these figures. Besides that, in terms of percentage, the following results based on Figs. 3, 4, 5, 6, 7, 8, 9, 10, 11 and 12 are obtained as

1) When $\alpha$ varies from 0.2 to 0.8, the decrement for velocity of second grade fluid is 20.50 % (primary) and 5.50 % (secondary) then increment about 5.00

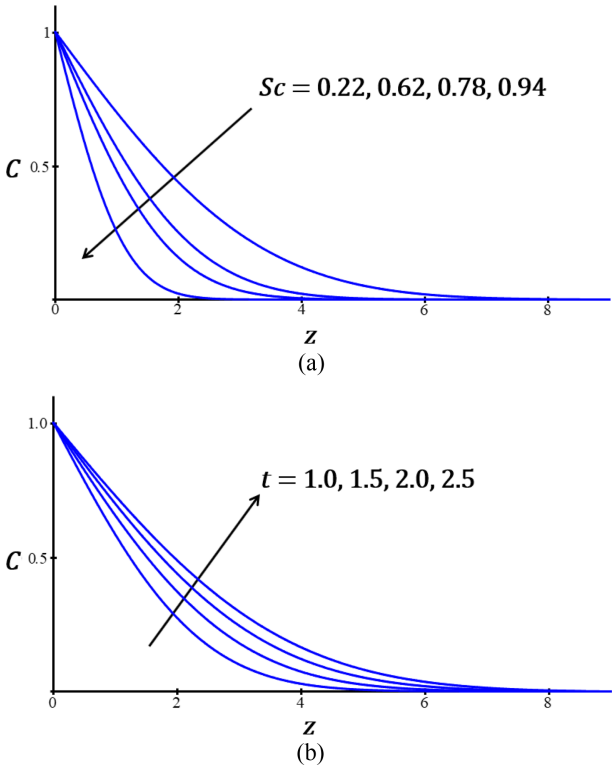


**Fig. 14.** (Color online) Concentration profiles for different values of (a) *Sc* with $t$ = 1.00 and (b) $t$ with *Sc* = 0.60.

% (primary) and 6.50 % (secondary) for cosine respectively.

2) When $\alpha$ varies from 0.2 to 0.8, the decrement for velocity of second grade fluid is 13.75 % (primary) and 6.50 % (secondary) then increment about 5.00 % (primary) and 1.00 % (secondary) for sine respectively.
3) When *Gr* varies from 0 to 8.5, the increment for velocity of second grade fluid is 20.15 % (primary) and 2.60 % (secondary) for cosine whereas 17.85 % (primary) and 2.65 % (secondary) for sine, respectively.
4) When *Gm* varies from 0 to 8.5, the increment for velocity of second grade fluid is 73.05 % (primary) and 15.85 % (secondary) for cosine whereas 38.90 % (primary) and 15.60 % (secondary) for sine, respectively.
5) When Pr varies from 1.0 to 50, the decrement for velocity of second grade fluid is 37.55 % (primary) and 7.25 % (secondary) for cosine whereas 28.90 % (primary) and 7.10 % (secondary) for sine, respectively.
6) When *Sc* varies from 0.22 to 0.94, the decrement for velocity of second grade fluid is 4.80 % (primary) and 1.6 % (secondary) for cosine whereas 2.25 % (primary) and 1.4 % (secondary) for sine, respectively.
7) When $M$ varies from 0 to 0.8, the decrement for velocity of second grade fluid is 10.95 % (primary) and 5.15 % (secondary) for cosine whereas 5.95 % (primary) and 2.50 % (secondary) for sine, respectively.
8) When $K$ varies from 1 to 12, the increment for velocity of second grade fluid is 20.15 % (primary) and 10.40 % (secondary) for cosine whereas 12.15 % (primary) and 5.65 % (secondary) for sine, respectively.
9) When $t$ varies from 1.0 to 2.5, the increment for velocity of second grade fluid is 50.00 % (primary) and 51.00 % (secondary) for cosine whereas 77.50 % (primary) and 22.50 % (secondary) for sine, respectively.
10) When $U_0$ varies from 2 to 5, the increment for velocity of second grade fluid is 53.55 % (primary) and 18.10 % (secondary) for cosine whereas 98.65 % (primary) and 11.65 % (secondary) for sine, respectively.
11) When $\omega t$ varies from 0 to $\pi/2$, the decrement for velocity of second grade fluid is 57.45 % (primary) and 8.55 % (secondary) for cosine whereas increment about 40.55 % (primary) and 8.70 % (secondary) for sine, respectively.

Thus, it can be said that *Gm*, $t$, $U_0$ and $\omega t$ cause a significant impact on the velocity profiles for double diffusion of second grade fluid in non-coaxial rotation. For parameter *Gm*, physically, mass is particle that transfers heat energy from one place to another place. Therefore, mass acts as a medium to transfer heat, thus the concentration of fluid increases due to the increase of the amount

**Table 5.** Variation of Nusselt number *Nu* (39) for different parameters $t$ and Pr.

| $t$ | Pr | *Nu* |
|---|---|---|
| 1.00 | 6.20 | 1.405 |
| 2.00 | 6.20 | 0.993 |
| 1.00 | 7.20 | 1.514 |

**Table 6.** Variation of Sherwood number *Sh* (40) for different parameters $t$ and *Sc*.

| $t$ | *Sc* | *Sh* |
|---|---|---|
| 1.00 | 0.60 | 0.437 |
| 2.00 | 0.60 | 0.309 |
| 1.00 | 0.96 | 0.553 |

**Table 7.** Variation of skin friction (41) for different parameters in primary and secondary velocities.

| $t$ | Pr | $Gr$ | $\omega$ | $U_0$ | $M$ | $K$ | $Gm$ | $Sc$ | $\alpha$ | Primary | Secondary |
|---|---|---|---|---|---|---|---|---|---|---|---|
| 1.00 | 5.00 | 5.00 | $\pi/3$ | 3.00 | 0.20 | 2.00 | 5.00 | 0.62 | 0.20 | -5.503 | -1.254 |
| 1.50 | 5.00 | 5.00 | $\pi/3$ | 3.00 | 0.20 | 2.00 | 5.00 | 0.62 | 0.20 | -8.123 | -1.449 |
| 1.00 | 7.20 | 5.00 | $\pi/3$ | 3.00 | 0.20 | 2.00 | 5.00 | 0.62 | 0.20 | -5.131 | -1.212 |
| 1.00 | 5.00 | 8.50 | $\pi/3$ | 3.00 | 0.20 | 2.00 | 5.00 | 0.62 | 0.20 | -6.665 | -1.383 |
| 1.00 | 5.00 | 5.00 | $\pi/2$ | 3.00 | 0.20 | 2.00 | 5.00 | 0.62 | 0.20 | -8.062 | -0.953 |
| 1.00 | 5.00 | 5.00 | $\pi/3$ | 4.00 | 0.20 | 2.00 | 5.00 | 0.62 | 0.20 | -5.523 | -1.536 |
| 1.00 | 5.00 | 5.00 | $\pi/3$ | 3.00 | 0.40 | 2.00 | 5.00 | 0.62 | 0.20 | -5.394 | -1.202 |
| 1.00 | 5.00 | 5.00 | $\pi/3$ | 3.00 | 0.20 | 5.00 | 5.00 | 0.62 | 0.20 | -5.791 | -1.428 |
| 1.00 | 5.00 | 5.00 | $\pi/3$ | 3.00 | 0.20 | 2.00 | 8.50 | 0.62 | 0.20 | -7.486 | -1.671 |
| 1.00 | 5.00 | 5.00 | $\pi/3$ | 3.00 | 0.20 | 2.00 | 5.00 | 0.94 | 0.20 | -5.277 | -1.146 |
| 1.00 | 5.00 | 5.00 | $\pi/3$ | 3.00 | 0.20 | 2.00 | 5.00 | 0.62 | 0.40 | -6.014 | -1.295 |

**Table 8.** Variation of skin friction (42) for different parameters in primary and secondary velocities.

| $t$ | Pr | $Gr$ | $\omega$ | $U_0$ | $M$ | $K$ | $Gm$ | $Sc$ | $\alpha$ | Primary | Secondary |
|---|---|---|---|---|---|---|---|---|---|---|---|
| 1.00 | 5.00 | 5.00 | $\pi/3$ | 3.00 | 0.20 | 2.00 | 5.00 | 0.62 | 0.20 | -2.019 | -1.079 |
| 1.50 | 5.00 | 5.00 | $\pi/3$ | 3.00 | 0.20 | 2.00 | 5.00 | 0.62 | 0.20 | -3.404 | -1.959 |
| 1.00 | 7.20 | 5.00 | $\pi/3$ | 3.00 | 0.20 | 2.00 | 5.00 | 0.62 | 0.20 | -1.828 | -1.038 |
| 1.00 | 5.00 | 8.50 | $\pi/3$ | 3.00 | 0.20 | 2.00 | 5.00 | 0.62 | 0.20 | -3.181 | -1.208 |
| 1.00 | 5.00 | 5.00 | $\pi/2$ | 3.00 | 0.20 | 2.00 | 5.00 | 0.62 | 0.20 | -2.421 | -1.281 |
| 1.00 | 5.00 | 5.00 | $\pi/3$ | 4.00 | 0.20 | 2.00 | 5.00 | 0.62 | 0.20 | -0.877 | -1.304 |
| 1.00 | 5.00 | 5.00 | $\pi/3$ | 3.00 | 0.40 | 2.00 | 5.00 | 0.62 | 0.20 | -1.892 | -1.046 |
| 1.00 | 5.00 | 5.00 | $\pi/3$ | 3.00 | 0.20 | 5.00 | 5.00 | 0.62 | 0.20 | -2.449 | -1.215 |
| 1.00 | 5.00 | 5.00 | $\pi/3$ | 3.00 | 0.20 | 2.00 | 8.50 | 0.62 | 0.20 | -4.001 | -1.497 |
| 1.00 | 5.00 | 5.00 | $\pi/3$ | 3.00 | 0.20 | 2.00 | 5.00 | 0.94 | 0.20 | -1.793 | -0.971 |
| 1.00 | 5.00 | 5.00 | $\pi/3$ | 3.00 | 0.20 | 2.00 | 5.00 | 0.62 | 0.40 | -1.915 | -1.039 |

of mass in fluid flow. Then, during the change of time, the flow gets energy from an external source. This external source is produced by a buoyancy force that will increase the velocity when time is increased. Lastly, parameters $U_0$ and $\omega t$ are the forced convection of boundary condition that enhances the movement of fluid flow and increase the velocity profiles.

Results for Nusselt (39) and Sherwood (40) numbers are presented in Tables 5 to 6. It can be seen that, the behaviors of parameters for Nusselt and Sherwood number are always opposite to that of velocity profiles. Finally,the numerical values of skin friction (43-44) are shown in Tables 7 to 8. In all these tables, each of the parameters has been compared with the first row of corresponding table. The bold number in each table shows the variation of that parameter. It is found that the behavior of skin friction for each parameter shows a quite opposite effect to the velocity of the fluid. For example, when $Gr$ increases, the skin friction decreases, whereas the velocity increases, as discussed previously.

## 5. Conclusion

An exact solution for unsteady free convection flow of MHD second fluid due to non-coaxial rotation over an oscillating vertical disk with isothermal temperature and constant mass diffusion is obtained by using the Laplace transform method. Effects of various embedded parameters on velocity are studied graphically in various plots. Results of Nusselt number, Sherwood number and skin friction are computed in different tables. The disk and fluid are rotating with uniform angular velocity which is equal to 1 in the present computations. The following main results are concluded from this study:

1) Both primary and secondary velocities increase with increasing $Gr$, $Gm$, $K$, $t$, $U_0$ and $\omega t$ (sine).
2) Both primary and secondary velocities decrease with increasing $M$, Pr, $Sc$ and $\omega t$ (cosine).
3) Both temperature and concentration profiles increase with increasing $t$.
4) Both temperature and concentration profiles decrease with increasing Pr and $Sc$.

5) Skin friction increases with increasing values of $M$, Pr, $Sc$ and $\omega t$ (cosine) whereas it decreases with increasing values of $Gr$, $Gm$, $K$, $t$, $U_0$ and $\omega t$ (sine).
6) In limiting sense for validation, the present results are good agreement with published result by Guria [10] and numerical Stehfest-Algorithm.

## Acknowledgment

The authors would like to acknowledge Ministry of Education (MOE) and Research Management Centre-UTM, Universiti Teknologi Malaysia (UTM) for the financial support through vote numbers 5F004, 07G70, 07G72, 07G76 and 07G77 for this research.

## References

[1] R. Berker, (English edition), Handbook of Fluid Dynamics, Vol. VIII/3, Springer, Berlin, (1963) 87.
[2] J. Coirier, J. de Mcanique **11**, 317 (1972).
[3] M. Erdogan, Trans. ASME J. Appl. Mech. **43**, 203 (1976).
[4] S. N. Murthy and R. K. P. Ram, Int. J. Engng. Sci. **16**, 943 (1978).
[5] K. R. Rajagopal, Arch. Rat. Mech. Anal. **79**, 39 (1982).
[6] S. R. Kasiviswanathan and A. R. Rao, Int. J. Engng. Sci. **25**, 1419 (1987).
[7] M. Guria, S. Das, and R. N. Jana, Int. J. Non-Linear Mech. **42**, 1204 (2007).
[8] S. Asghar, K. Hanif, and T. Hayat, Meccanica **42**, 141 (2007).
[9] T. Hayat, R. Ellahi, and S. Asghar, Chem. Eng. Comm. **195**, 958 (2008).
[10] M. Guria, A. K. Kanch, S. Das, and R. N. Jana, Meccanica **45**, 23 (2010).
[11] S. L. Maji, G. Manna, M. Guria, and R. N. Jana, Chem. Eng. Comm. **197**, 791 (2010).
[12] A. Q. Mohamad, I. Khan, Z. Ismail, and S. Shafie, SpringerPlus **5**, 1 (2016).
[13] A. Q. Mohamad, I. Khan, S. Shafie, Z. M. Isa, and Z. Ismail, Neural Comput. & Applic. 1 (2017).
[14] B. D. Coleman and W. Noll, Archive for Rational Mechanics and Analysis **6**, 355 (1960).
[15] S. A. Samiulhaq, D. Vieru, I. Khan, and S. Shafie, PLoS ONE **9**, 1 (2014).
[16] M. Imran, M. Imran, and C. Fetecau, Communications in Numerical Analysis **2014**, 1 (2014).
[17] A. A. Zafar, D. Vieru, and S. Akhtar, Journal of Prime Research in Mathematics **10**, 45 (2015).
[18] A. Khan and G. Zaman, Journal of Applied Fluid Mechanics **9**, 3127 (2016).
[19] M. VeeraKrishna and G. S. Reddy, IOP Conf. Series: Materials Science and Engineering **149**, 1 (2016).
[20] Z. Ismail, I. Khan, A. Q. Mohamad, and S. Shafie, Defect and Diffusion Forum **362**, 100 (2015).
[21] D. Vieru, M. A. Imran, and A. Rauf, Heat Transfer Research **46**, 713 (2015).
[22] A. Q. Mohamad, I. Khan, and S. Shafie, AIP Conference Proceedings **1750**, 1 (2016).
[23] A. Q. Mohamad, I. Khan, Z. Ismail, N. A. M. Zin, and Sharidan Shafie, AIP Conference Proceedings **1775**, 1 (2016).
[24] T. Hayat, R. Ellahi, S. Asghar, and A. M. Siddiqui, Applied Mathematical Modelling **28**, 591 (2004).
[25] T. Hayat, R. Ellahi, and S. Asghar, Chem. Eng. Comm. **194**, 37 (2007).
[26] A. Q. Mohamad, I. Khan, N. A. M. Zin, Z. M. Isa, S. Shafie, and Z. Ismail, AIP Conference Proceedings **1830**, 1 (2017).
[27] H. Stehfest, Commun ACM **13**, 47 (1970).
[28] H. Villinger, Geophysics **50**, 1581 (1985).